crystals

MDPI

Article

Coordination of a Pyrazole Functionalized Acetylacetone to the Coinage Metal Cations: An Unexpected Packing Similarity and a Trinuclear Cu^{II}/Au^{I} Complex

Steven van Terwingen [1], Ben Ebel [1], Noah Nachtigall [1] and Ulli Englert [1,2,*]

[1] Institute of Inorganic Chemistry, RWTH Aachen University, Landoltweg 1, 52074 Aachen, Germany; steven.vanterwingen@ac.rwth-aachen.de (S.v.T.); ben.ebel@rwth-aachen.de (B.E.); noah.nachtigall@ac.rwth-aachen.de (N.N.)

[2] Key Laboratory of Chemical Biology and Molecular Engineering of the Education Ministry, Shanxi University, 92 Wucheng Road, Taiyuan 030006, China

* Correspondence: ullrich.englert@ac.rwth-aachen.de; Tel.: +49-241-80-90064

Abstract: The heteroditopic molecule HacacMePz combines a Pearson hard acetylacetone donor site with a softer trimethylpyrazole and shows site selectivity towards the coinage metal cations. The coordination of the N donor function was achieved towards Ag^{I} and Au^{I}, leading to the salt $[Ag(HacacMePz)_2]PF_6$ (**1**) and the neutral complex [AuCl(HacacMePz)] (**2**). In either case, linear coordination about the coinage metal cation is observed. Interestingly, both complexes crystallize in space group *Pbca* with similar cell parameters. The two solids do not qualify as isostructural, albeit being closely related in real and reciprocal space. To probe the ligand's ability for the envisaged synthesis of bimetallic coordination polymers, the mixed-metal Cu^{II}/Au^{I} complex $[Cu(acacMePzAuCl)_2]$ (**3**) was obtained. In this mixed-metal oligomer, the central Cu^{II} cation adopts a square planar coordination environment with two O,O′-coordinated $acacMePz^{-}$ ligands, whose softer N donor sites are saturated with a AuCl moiety.

Keywords: packing similarity; ditopic ligand; bimetallic coordination; coinage metal cations

check for updates

Citation: van Terwingen, S.; Ebel, B.; Nachtigall, N.; Englert, U. Coordination of a Pyrazole Functionalized Acetylacetone to the Coinage Metal Cations: An Unexpected Packing Similarity and a Trinuclear Cu^{II}/Au^{I} Complex. *Crystals* **2022**, *12*, 984. https://doi.org/10.3390/cryst12070984

Academic Editor: Elizabeth A. Hillard

Received: 29 June 2022
Accepted: 12 July 2022
Published: 15 July 2022

1. Introduction

In recent years, the interest in organic–inorganic hybrid materials has flourished. Coordination polymers (CPs) are a subclass of the aforementioned, in which metal cations are bridged by ligands periodically in at least one dimension [1]. CPs are promising candidates for the increasing demand for tailored materials: the seemingly inexhaustible combinations of organic ligands with different metal species offer a huge playground for the modern physicist, chemist and material scientist. Gas sorption [2–4] and separation [5,6], catalysis [7–9] or luminescence [10–12] are only a few of the potentially useful properties of CPs. Often, these desirable characteristics directly arise from the metal species used, and thus it could be advantageous to incorporate more than one metal cation to combine their properties in a joint material. Our group utilizes heteroditopic ligands to enable a selectivity in this otherwise statistical [13] construction process (Figure 1) [14–17].

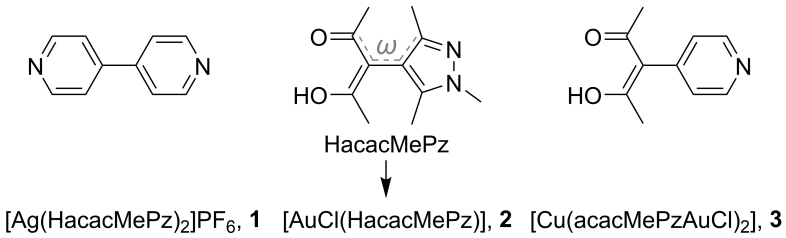

Figure 1. Structures of homoditopic 4,4′-bipyridine (**left**) and heteroditopic ligands 3-(1,3,5-trimethyl-1*H*-pyrazol-4-yl)acetylacetone (HacacMePz, (**center**)) and 3-(4-pyridyl)acetylacetone (**right**) [18,19].

The important angle ω has been marked in gray, and a synopsis of all compounds discussed in this work is given below.

While the two binding sites of 4,4′-bipyridine are equivalent and do not exhibit selectivity towards specific metals, each of the inequivalent donors of the functionalized acetylacetones in Figure 1 preferably binds to specific cations. This selectivity is based on different Pearson hardnesses [20,21] of the ligand's donor sites and, vice versa, of the metal cations used. Recently, we reported the ditopic coordination chemistry of the pyrazole functionalized acetylacetone (HacacMePz, Figure 1 center) for the selective construction of bimetallic CPs. After deprotonation, the diketonate moiety acted as a chelating ligand towards small and notoriously hard Fe^{III} cations, whereas the N donor site selectively attached to larger cations carrying a lower charge, e.g., Hg^{II} or Ag^{I} [17]. In this study, we address cations with less pronounced differences in their Pearson hardness and focus on a single group in the periodic table, namely, the coinage metals. The elements in group 11 form continuous solid solutions [22]. We report here that the cations of the coinage metals selectively form coordination compounds with HacacMePz. Ag^{I} and Au^{I} afford N-coordinated building blocks suitable for further crosslinking, and ditopic coordination of the ligand leads to a bimetallic trinuclear Cu^{II}/Au^{I} complex.

2. Materials and Methods

All chemicals were purchased from common vendors and used without further purification. 3-(1,3,5-Trimethyl-1*H*-pyrazol-4-yl)acetylacetone [17] and [AuCl(THT)] [23] were synthesized using procedures published before. ATR FT IR spectra were obtained with a Shimadzu IRSpirit with a QATR-S ATR unit equipped with a diamond prism. The magnetic resonance spectrum was measured using a Bruker Avance II UltrashieldT11 plus 400 instrument (400 MHz, referenced to $SiMe_4$).

2.1. Synthesis and Crystallization of [Ag(HacacMePz)$_2$]PF$_6$, **1**

HacacMePz (41.6 mg, 0.2 mmol, 2.0 eq.) and $AgPF_6$ (25.3 mg, 0.1 mmol, 1.0 eq.) were separately dissolved in ethyl acetate (2 mL each). The two clear solutions were combined. The solution was stored at 4 °C, and colorless block-shaped crystals suitable for SCXRD formed overnight. Yield: 51.3 mg (77 %). IR (ATR, $\tilde{\nu}/cm^{-1}$): 2965 (vw), 2925 (vw), 2359 (w), 2344 (w), 1601 (m), 1560 (m), 1488 (m), 1421 (m), 1389 (s), 1319 (m), 1301 (m), 1276 (m), 1136 (m), 994 (m), 914 (m), 843 (vs), 818 (vs), 715 (m), 668 (w), 637 (vw), 574 (w), 555 (vs), 495 (m), 475 (w). CHN: anal. calcd. for $C_{22}H_{32}AgF_6N_4O_4P$: C 39.5 %, H 4.8 %, N 8.4 %; found: C 39.7 %, H 4.8 %, N 8.6 %. PXRD performed on the bulk material allowed us to recognize the presence of a minor crystalline impurity (Figure S1).

2.2. Synthesis and Crystallization of [AuCl(HacacMePz)], **2**

HacacMePz (11.2 mg, 0.06 mmol, 1.2 eq.) and [AuCl(THT)] (16.0 mg, 0.05 mmol, 1.0 eq.) were dissolved in deuterated chloroform (1 mL). Colorless block-shaped crystals suitable for SCXRD were obtained from $CDCl_3$ at 4 °C by slow gas diffusion of *n*-pentane into the solution. Yield: 16.2 mg (74 %). ^{1}H NMR ($CDCl_3$, 400 MHz): δ 16.86 (s, 1H), 3.78 (s, 3H), 2.13 (s, 6H), 1.85 (s, 6H) ppm. IR (ATR, $\tilde{\nu}/cm^{-1}$): 2962 (w), 2920 (w), 1597 (s), 1560 (s), 1485 (s), 1414 (vs), 1389 (vs), 1365 (s), 1275 (s), 1220 (s), 992 (s), 917 (s), 714 (m), 670 (m), 535 (m), 474 (m). CHN: anal. calcd. for $C_{11}H_{16}AuClN_2O_2$: C 30.0 %, H 3.7 %, N 6.4 %; found: C 33.0 %, H 4.0 %, N 7.0 %. Phase purity was confirmed via PXRD (Figure S2).

2.3. Synthesis and Crystallization of [Cu(acacMePzAuCl)$_2$], **3**

HacacMePz (5.2 mg, 0.025 mmol, 2.0 eq.), $Cu(OAc)_2 \cdot H_2O$ (2.7 mg, 0.0125 mmol, 1.0 eq.) and [AuCl(THT)] (7.7 mg, 0.025 mmol, 2.0 eq.) were separately dissolved in acetonitrile (2 mL) each. The HacacMePz solution was combined with the $Cu(OAc)_2$ solution; then, the [AuCl(THT)] solution was added. The solution was stored at −25 °C. Eventually, after 11 d, light blue plate-shaped crystals suitable for SCXRD were obtained and isolated.

Yield: 6.8 mg (56 %). IR (ATR, $\tilde{\nu}$/cm^{-1}): 2998 (vw), 2930 (w), 2359 (w), 2248 (w), 1585 (vs), 1549 (m), 1416 (m), 1368 (vs), 1281 (s), 1036 (vs), 974 (m), 927 (m), 851 (w), 723 (m), 714 (w), 685 (m), 633 (m), 464 (vs). Microanalysis of the dried bulk: CHN: anal. calcd. for $C_{22}H_{30}AuCl_2CuN_4O_4$: C 28.0 %, H 3.2 %, N 5.9 %; found: C 26.0 %, H 3.6 %, N 5.4 %. PXRD confirms that the majority of the bulk material corresponds to the phase identified by SCXRD; however, a few reflections that cannot be attributed to **3** are visible in the diffractogram (Figure S2). Measurement under acetonitrile and perfluorinated oil was intended to reduce desolvation but did not improve the diffractogram.

2.4. Structure Determinations

For **1**, intensity data were collected on a STOE STADIVARI goniometer (STOE & Cie GmbH, Darmstadt, Germany; location of the instrument: Institute of Inorganic Chemistry, RWTH Aachen University) equipped with a DECTRIS Pilatus 200K area detector, GeniX 3D HF Mo microsource (λ = 0.710 73 Å, multilayer optics). Temperature was maintained with an Oxford Cryostream 800 instrument (Oxfordshire, UK). Data were collected and integrated with the X-Area program package [24]. Scaling and multi-scan absorption correction were applied with LANA [25].

For **2** and **3**, intensity data were collected on a Bruker D8 goniometer (Bruker AXS, Madison, USA; location of the instrument: Institute of Inorganic Chemistry, RWTH Aachen University) equipped with an APEX CCD area detector, Incoatec microsource with Mo-K$_\alpha$ radiation (λ = 0.710 73 Å, multilayer optics). Temperature was maintained with an Oxford Cryostream 700 instrument (Oxfordshire, UK). Data were collected with SMART [26] and were integrated with SAINT+ [27]. Scaling and multi-scan absorption correction were applied with SADABS [28].

The structures were solved by intrinsic phasing with SHELXT-2014/5 [29]; full-matrix least squares refinements against F^2 were carried out with SHELXL-2019/2 [30]. Non-H atoms were refined anisotropically. If possible, protic H atoms were located from difference Fourier synthesis maps, and their positional coordinates were refined freely. Other H atoms were placed in idealized positions and refined as riding. Isotropic displacement parameters for H atoms were constrained to multiples of their parent atoms, namely, U_{iso}(H) = 1.5U_{eq}(C,N,O) for methyl/protic hydrogen and U_{iso}(H) = 1.2U_{eq}(C) for other H atoms.

2.5. Powder Diffraction and Rietveld Refinement

Powder diffractograms were recorded on flat samples at room temperature using a STOE STADI-P diffractometer (STOE & Cie GmbH, Darmstadt, Germany; location of the instrument: Institute of Inorganic Chemistry, RWTH Aachen University) with Guinier geometry (Cu-K$_{\alpha1}$, λ = 1.540 59 Å, Johann germanium monochromator, STOE image plate detector IP-PSD, 0.005° step width in 2θ). Rietveld refinements for **1** and **2** were carried out with the program GSAS-II [31] using a pseudo-Voigt profile function. Residual values for **1**: wR_P = 0.2680, wR_B = 0.3980 for 496 Bragg reflections (3835 data points) and 5 refined parameters. Residual values for **2**: wR_P = 0.1337, wR_B = 0.1764 for 465 Bragg reflections (3835 data points) and 12 refined parameters.

3. Results

A classic candidate for the selective coordination of the rather Pearson soft pyrazole N site of HacacMePz is Ag^I. In a preceding article, we reported the $AgNO_3$ complex [Ag(NO_3)(HacacMePz)$_2$], in which the nitrate anion is still coordinating and prevents a strictly linear arrangement of the pyrazole moieties [17]. Here, we disclose the complex of HacacMePz with $AgPF_6$. The PF_6^- anion is less coordinating and more likely to form a bis-pyrazolyl silver(I) cationic complex than coordinating anions such as NO_3^- [32]. The compound [Ag(HacacMePz)$_2$]PF_6 (**1**) crystallizes in the orthorhombic space group *Pbca* with $Z = 4$ (Figure 2).

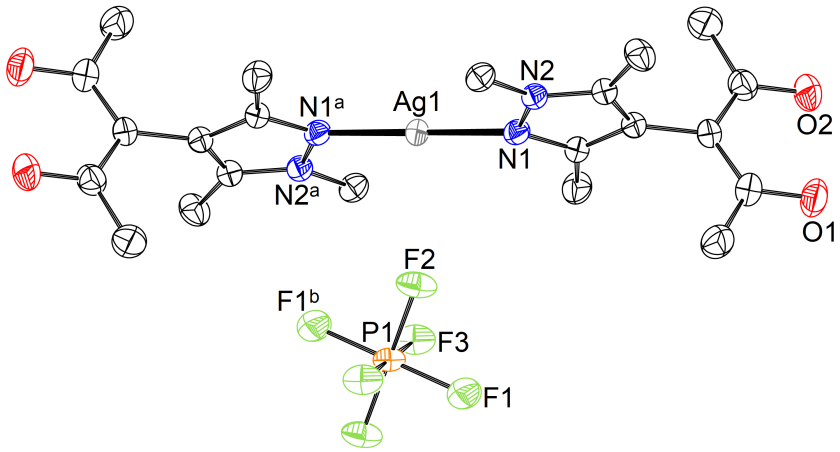

Figure 2. Displacement ellipsoid plot [33] of **1** (70 % probability, hydrogen omitted). Selected distances and angles (Å, °): Ag1–N1 2.125(2), Ag1···F2 2.9444(15), ω 84.84(12). Symmetry operations: a = $1-x, -y, -z$; b = $-x, -y, -z$.

The cationic $[AgPz_2]^+$ moieties are linear for reasons of symmetry, with the Ag^I cation occupying the inversion center on Wyckoff position 4*b*. The $PF_6{}^-$ anion is located on the other inversion center on Wyckoff position 4*a*. The closest contact between the $PF_6{}^-$ and the adjacent bis-pyrazolyl complex amounts to 2.9444(15) Å. Interestingly, no Ag^I complex of unsubstituted trimethylpyrazole has been reported to this date.

The reaction of HacacMePz with the precursor [AuCl(THT)] leads to the linear complex [AuCl(HacacMePz)] (**2**), which crystallizes in the orthorhombic space group *Pbca* with $Z = 8$ (Figure 3).

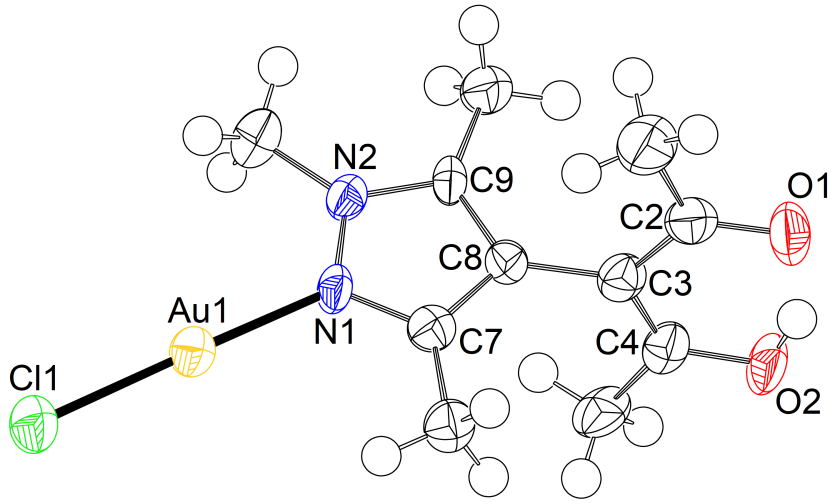

Figure 3. Displacement ellipsoid plot [33] of **2** (90 % probability). Selected intramolecular distances and angles (Å, °): Au1–Cl1 2.2446(13), Au1–N1 2.011(4), Cl1–Au1–N1 178.15(12), ω 79.0(3).

As expected, the Cl–Au–N angle is close to linear with 178.15(12)°. The enol hydrogen is clearly localized, with a C–O single bond (1.303(6) Å) and a C=O double bond (1.265(6) Å). While there are many reports of aurophilic interactions in the crystal structures of AuCl complexes [34–38], **2** does not exhibit this behavior. The steric bulk of the methyl substituents might impede a closer approach; alternatively, a weak aurophilic contact might be overcome by a more suitable packing.

Copper(II) acetate is sufficiently basic to deprotonate the acetylacetone site of the Au^I building block **2**. If concentration and temperature are suitably chosen, single crystals of the compound $[Cu(acacMePzAuCl)_2] \cdot 2\,MeCN$ (**3** · 2 MeCN) are obtained (Figure 4). It crystallizes as a discrete complex in the monoclinic space group $P2_1/c$ with $Z = 2$.

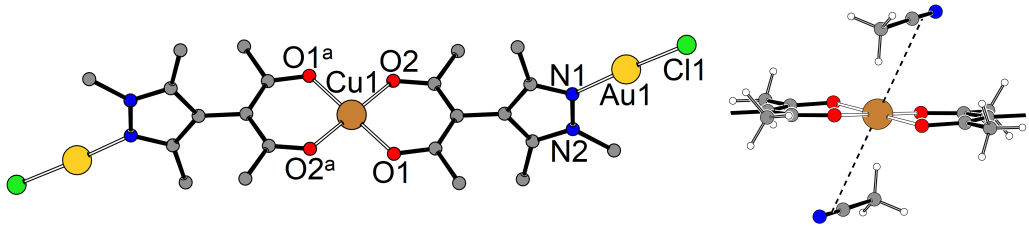

Figure 4. Left: PLUTON plot [33] of the discrete complex in **3** · 2 MeCN (solvent MeCN omitted). Right: Coordination sphere around Cu1 with side-on coordinated solvent MeCN molecules. Selected intramolecular distances and angles (Å, °): Au1–Cl1 2.2458(19), Au1–N1 2.010(6), Cu1–O1 1.883(5), Cu1–O2 1.896(5), Cl1–Au1–N1 177.12(17), ω 71.7(4). Symmetry operation: a = $2-x, 1-y, 1-z$.

The central Cu1 ion is located on the inversion center with Wyckoff letter 2*a* and adopts square planar coordination with two chelating acetylacetonate moieties of HacacMePz. Both N donor sites of the acacMePz$^-$ ligand coordinate a AuCl moiety in a linear fashion, with an angle of 177.12(17)°. Interestingly, the ω angle deviates from orthogonality and amounts to the rather unfavorable value of 71.7(4)° [17]. Two symmetry-equivalent acetonitrile molecules come close to the central Cu1 ion, albeit not in the regular linear N donor fashion. The N and C atom of each nitrile group are located at a distance of about 3.7 Å with respect to Cu1 to engage in a very long side-on coordination. This is larger than the sum of their van der Waals radii, but has an effect on the C≡N stretching vibrations observed via IR spectroscopy. The latter undergoes a minor red shift from 2253 cm^{-1} to 2248 cm^{-1}, indicating a slightly weakened C≡N bond as a result of the weak interaction with the Cu^{II} cation. No further unexpectedly short intermolecular contacts were encountered.

4. Discussion

4.1. Surprising Packing Similarity of **1** *and* **2**

A comparison of the powder diffractograms of the gold(I) complex **2** with that for the $AgPF_6$ complex **1** reveals surprising similarities (Figure 5).

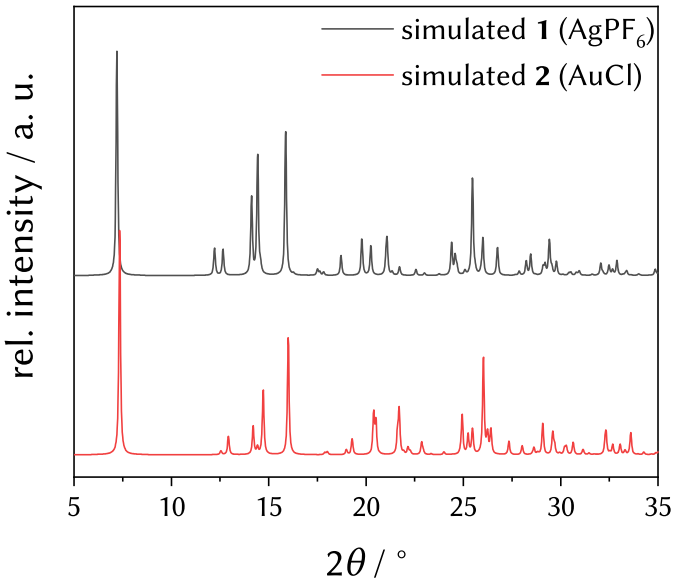

Figure 5. Simulated powder X-ray diffractograms of **1** (black) and **2** (red) in comparison.

Both structures crystallize in the same space group *Pbca* with similar lattice parameters, although with *a* and *b* being anti-parallel to each other in the two structures. They also exhibit a different number of molecules per unit cell: the gold(I) complex crystallizes with $Z = 8$ and the molecule in general position, whereas the silver(I) complex exhibits $Z = 4$ with the Ag^I ion on a center of inversion. The Au^I ion in **2** is shifted in *b* direction for about

$^{b}/_{4}$. A close inspection of the two structures shows they can indeed be superimposed to show a similar packing motif if the unit cells are slightly shifted (Figure 6).

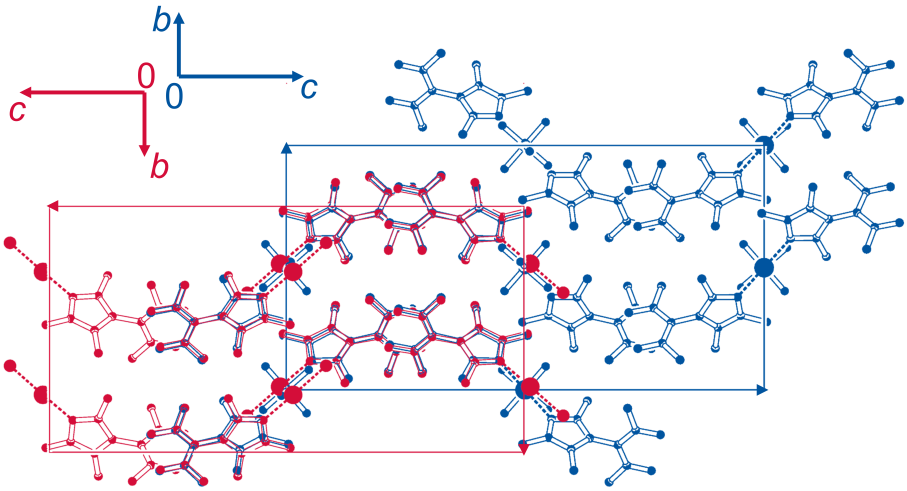

Figure 6. Overlay plot [33] of the unit cells of **2** (red) and **1** (blue) (hydrogen omitted), view along *a*.

In the resulting overlay, the positions of Ag^{I} ions and PF_6^- anions formally coincide with Au^{I} ions in the alternative structure. Do our compounds **1** and **2** qualify as *isostructural*? No, because it would require both similar stoichiometries of the two crystalline substances and equivalent occupation of special positions. But what about *isomorphism*? According to the IUCr dictionary [39,40], isomorphous structures need to exhibit three characteristics:

> Two crystals are said to be isomorphous if (a) both have the same space group and unit-cell dimensions and (b) the types and the positions of atoms in both are the same except for a replacement of one or more atoms in one structure with different types of atoms in the other (diadochy), such as heavy atoms, or the presence of one or more additional atoms in one of them (isomorphous addition). Isomorphous crystals can form solid solutions.

The first condition is obviously fulfilled, but the unit cell shift of $^{b}/_{4}$ required for efficient overlay maps a special position in **1** on a general position in **2**. Such relationships are difficult if not impossible to classify. A quick search in the CSD [41] reveals that there are 67 other orthorhombic structures with similar lattice parameters. Quite obviously, this leads to similarities in the reciprocal space and similar line positions in the diffraction patterns. If heavy atoms occupy special or pseudo-special positions in these structures, the contribution of light atoms to reflection intensities may be minor, and the overall X-ray powder diffractograms may appear to be similar. As an example the simulated powder patterns of **1** and a structurally unrelated Pd^{II} complex (refcode DOXMEL [42]) are compared in Figure 7. DOXMEL has been chosen quite arbitrarily for comparison, with similar lattice parameters as **1** and the presence of a heavy atom as the only criterion.

Despite their apparent similarity in reciprocal space, the real space match between **1** and DOXMEL is poor: the inversion center corresponding to Wyckoff position 4*a* is occupied by the Pd^{II} centers in DOXMEL and in **1** by the PF_6^- anions, and the remaining light atoms cannot be superimposed at all. With respect to our much closer related structures **1** and **2**, we therefore stick to the admittedly vague expression "packing similarity".

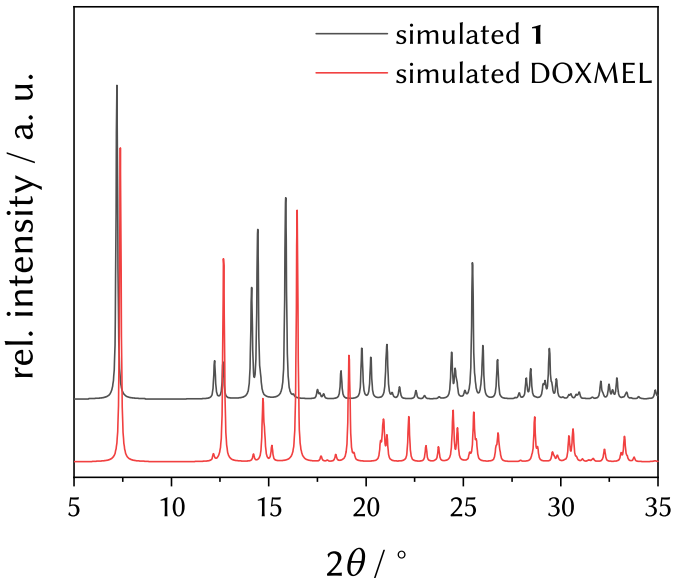

Figure 7. Simulated powder X-ray diffractograms of **1** (black) and DOXMEL (red) in comparison.

4.2. Structural Features of **3**

The coordination of the Au^I cations in **2** and **3** can be compared with chemically related species published earlier, namely, the gold complexes of trimethylpyrazol itself (XACQUQ) and an alternative substituted and potentially ditopic trimethylpyrazol (VAVMIS) (Table 1).

Table 1. Comparison of the coordination environment about the Au^I in **2**, **3** and two selected literature structures.

Compound	Au–Cl/Å	Au–N/Å	Cl–Au–N/°	ω/°
2	2.2446 (14)	2.011 (4)	178.15 (12)	79.0 (3)
3	2.2458 (19)	2.010 (6)	177.12 (17)	71.7 (4)
XACQUQ [43]	2.253 (2)	2.011 (7)	177.3 (2)	
VAVMIS [44]	2.2441 (17)	2.020 (4)	179.08 (11)	

The compounds in this comparison are essentially linear with similar metal–ligand distances. Aurophilic interactions are encountered in none of the above-mentioned AuCl complexes. As stated before, this might be attributed to the steric bulk of the methyl groups. The overlay plots of **3** with **2** and XACQUQ [43] reveal how similar the conformations in these complexes are (Figure 8).

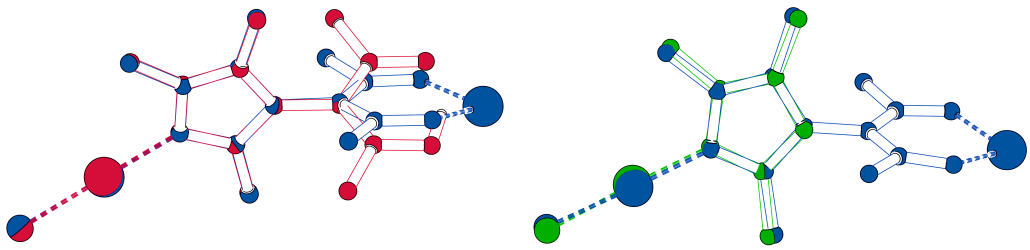

Figure 8. Overlay plots [33] of **3** (blue) with **2** (red) and with XACQUQ (green).

5. Conclusions

The packing similarities between the chemically quite different cationic Ag^I bis–ligand complex **1** and the neutral Au^I complex **2** are surprising yet difficult to classify. They are probably caused by the coincidence of several facts:

- Packing in each structure is dominated by the necessity to accommodate eight neutral N-coordinated HacacMePz ligands per unit cell; in either case, this involves the interaction of methyl H atoms with the pyrazole π-system;
- Both metal cations prefer a linear coordination;
- The distance between the non-coordinating counter-anion PF_6^- and the Ag^I cation is compatible with the Au···Au separation between neighboring molecules.

We are not aware of an established scientific term for such similarities.

With respect to CP design, the gold(I) complex **2** may be used as metalloligand towards a harder Cu^{II} cation in predictable geometry.

The resulting mixed-metal complex **3** qualifies as an oligonuclear compound rather than a coordination polymer. It proves, however, that our ligand is sufficiently selective to distinguish even chemically related cations from the same group based on their different Pearson hardness. Therefore, **3** paves the way to future extended and well-ordered mixed-metal structures. The next step towards a "real" polymer will imply a substitution of the terminal chlorido ligands attached to Au^I.

Supplementary Materials: The following supporting information can be downloaded at: https://www.mdpi.com/article/10.3390/cryst12070984/s1, Figure S1: Simulated (100 K and 280 K), Rietveld refined and experimental powder X-ray diffractograms of **1** (top). Three reflections that cannot be assigned to **1** have been marked with green arrows (bottom); Figure S2: Simulated and experimental powder X-ray diffractograms of **2** (top). Simulated and two experimental powder X-ray diffractograms (with and without oil) of **3** (bottom). The most obvious discrepancies have been marked with an arrow; Table S1: Crystal and refinement data for **1**, **2** and **3**.

Author Contributions: Conceptualization, S.v.T. and U.E.; methodology, S.v.T. and U.E.; software, S.v.T., N.N. and U.E.; validation, S.v.T. and U.E.; formal analysis, S.v.T., B.E. and N.N.; investigation, S.v.T., B.E. and N.N.; resources, U.E.; data curation, S.v.T.; writing—original draft preparation, S.v.T. and U.E.; writing—review and editing, S.v.T., B.E., N.N. and U.E.; visualization, S.v.T. and N.N.; supervision, U.E.; project administration, U.E.; funding acquisition, S.v.T and U.E. All authors have read and agreed to the published version of the manuscript.

Funding: This work was funded by a scholarship for doctoral students of the RWTH Graduiertenförderung to S.v.T.

Institutional Review Board Statement: Not applicable.

Informed Consent Statement: Not applicable.

Data Availability Statement: CCDC 2181634–2181636 contains the supplementary crystallographic data for this paper. These data can be obtained free of charge from The Cambridge Crystallographic Data Centre via www.ccdc.cam.ac.uk/data_request/cif.

Conflicts of Interest: The authors declare no conflict of interest. The funders had no role in the design of the study; in the collection, analyses, or interpretation of data; in the writing of the manuscript, or in the decision to publish the results.

Abbreviations

The following abbreviations are used in this manuscript:

CCDC	Cambridge Crystallographic Data Centre
CP	coordination polymer
CSD	Cambridge Structural Database
HacacMePz	3-(1,3,5-trimethyl-1*H*-pyrazol-4-yl)acetylacetone
IUCr	International Union of Crystallography
PXRD	powder X-ray diffraction
SCXRD	single-crystal X-ray diffraction
THT	tetrahydrothiophen

References

1. Batten, S.R.; Neville, S.M.; Turner, D.R. *Coordination Polymers: Design, Analysis and Application*, 1st ed.; RSC Publishing: Cambridge, UK, 2009.
2. Seki, K.; Takamizawa, S.; Mori, W. Design and Gas Adsorption Property of a Three-Dimensional Coordination Polymer with a Stable and Highly Porous Framwork. *Chem. Lett.* **2001**, *30*, 332–333. [CrossRef]
3. Lee, H.J.; Cho, W.; Jung, S.; Oh, M. Morphology-Selective Formation and Morphology-Dependent Gas-Adsorption Properties of Coordination Polymer Particles. *Adv. Mater.* **2009**, *21*, 674–677. [CrossRef]
4. Agarwal, R.A.; Mukherjee, S.; Sañudo, E.C.; Ghosh, S.K.; Bharadwaj, P.K. Gas Adsorption, Magnetism, and Single-Crystal to Single-Crystal Transformation Studies of a Three-Dimensional Mn(II) Porous Coordination Polymer. *Cryst. Growth Des.* **2014**, *14*, 5585–5592. [CrossRef]
5. Duan, J.; Jin, W.; Krishna, R. Natural gas purification using a porous coordination polymer with water and chemical stability. *Inorg. Chem.* **2015**, *54*, 4279–4284. [CrossRef] [PubMed]
6. Noro, S.; Ochi, R.; Inubushi, Y.; Kubo, K.; Nakamura, T. CH_4/CO_2 and CH_4/C_2H_6 gas separation using a flexible one-dimensional copper(II) porous coordination polymer. *Microporous Mesoporous Mat.* **2015**, *216*, 92–96. [CrossRef]
7. Yoo, S.K.; Ryu, J.Y.; Lee, J.Y.; Kim, C.; Kim, S.J.; Kim, Y. Synthesis, structure and heterogeneous catalytic activity of a coordination polymer containing tetranuclear Cu(ii)-btp units connected by nitrates. *Dalton Trans.* **2003**, 1454–1456. [CrossRef]
8. Hong, S.J.; Seo, J.S.; Ryu, J.Y.; Lee, J.H.; Kim, C.; Kim, S.J.; Kim, Y.; Lough, A.J. Structure and heterogeneous catalytic activity of a coordination polymer containing $Cu(NO_3)_2$ and units bridged alternatively by btp ligands (btp=2,6-bis(N′-1,2,4-triazolyl)pyridine). *J. Mol. Struct.* **2005**, *751*, 22–28. [CrossRef]
9. Zhou, Z.; He, C.; Yang, L.; Wang, Y.; Liu, T.; Duan, C. Alkyne Activation by a Porous Silver Coordination Polymer for Heterogeneous Catalysis of Carbon Dioxide Cycloaddition. *ACS Catal.* **2017**, *7*, 2248–2256. [CrossRef]
10. Chandler, B.D.; Coté, A.P.; Cramb, D.T.; Hill, J.M.; Shimizu, G.K.H. A sponge-like luminescent coordination framework via an Aufbau approach. *Chem. Commun.* **2002**, *17*, 1900–1901. [CrossRef]
11. Fenton, H.; Tidmarsh, I.S.; Ward, M.D. Luminescent silver(i) coordination networks based on bis-(3,5-dimethylpyrazolyl)naphthalene ligands. *CrystEngComm* **2011**, *13*, 1432–1440. [CrossRef]
12. Zhang, Y.Q.; Blatov, V.A.; Zheng, T.R.; Yang, C.H.; Qian, L.L.; Li, K.; Li, B.L.; Wu, B. A luminescent zinc(ii) coordination polymer with unusual (3,4,4)-coordinated self-catenated 3D network for selective detection of nitroaromatics and ferric and chromate ions: A versatile luminescent sensor. *Dalton Trans.* **2018**, *47*, 6189–6198. [CrossRef] [PubMed]
13. Şerb, M.D.; Speldrich, M.; Lueken, H.; Englert, U. Isomorphous Catena Transition Metal Squarates $[MII(C_4O_4)(dmso)_2(OH_2)_2]$ (M = Co, Mn) and Magnetic Investigation into their Solid Solution M = CoxMn1-x. *Z. Anorg. Allg. Chem.* **2011**, *637*, 536–542. [CrossRef]
14. Kondracka, M.; Englert, U. Bimetallic coordination polymers via combination of substitution-inert building blocks and labile connectors. *Inorg. Chem.* **2008**, *47*, 10246–10257. [CrossRef] [PubMed]
15. Merkens, C.; Englert, U. Ordered bimetallic coordination networks featuring rare earth and silver cations. *Dalton Trans.* **2012**, *41*, 4664–4673. [CrossRef]
16. Gildenast, H.; Nölke, S.; Englert, U. 3-(4-Methylthiophenyl)acetylacetone—Ups and downs of flexibility in the synthesis of mixed metal–organic frameworks. Ditopic bridging of hard and soft cations and site-specific desolvation. *CrystEngComm* **2020**, *22*, 1041–1049. [CrossRef]
17. van Terwingen, S.; Nachtigall, N.; Ebel, B.; Englert, U. N-Donor-Functionalized Acetylacetones for Heterobimetallic Coordination Polymers, the Next Episode: Trimethylpyrazoles. *Cryst. Growth Des.* **2021**, *21*, 2962–2969. [CrossRef]
18. Vreshch, V.D.; Chernega, A.N.; Howard, J.A.K.; Sieler, J.; Domasevitch, K.V. Two-step construction of molecular and polymeric mixed-metal Cu(Co)/Be complexes employing functionality of a pyridyl substituted acetylacetonate. *Dalton Trans.* **2003**, *9*, 1707–1711. [CrossRef]
19. Mackay, L.G.; Anderson, H.L.; Sanders, J.K.M. A platinum-linked porphyrin trimer and a complementary aluminium tris[3-(4-pyridyl)acetylacetonate] guest. *J. Chem. Soc., Perkin Trans.* **1995**, *1*, 2269. [CrossRef]
20. Pearson, R.G. Hard and Soft Acids and Bases. *J. Am. Chem. Soc.* **1963**, *85*, 3533–3539. [CrossRef]
21. Pearson, R.G. Hard and soft acids and bases, HSAB, part 1: Fundamental principles. *J. Chem. Educ.* **1968**, *45*, 581–587. [CrossRef]
22. Goodwin, F.; Guruswamy, S.; Kainer, K.U.; Kammer, C.; Knabl, W.; Koethe, A.; Leichtfried, G.; Schlamp, G.; Stickler, R.; Warlimont, H. Metals. In *Springer Handbook of Condensed Matter and Materials Data*; Martienssen, W., Warlimont, H., Eds.; Springer: Berlin/Heidelberg, Germany, 2005; Volume 2, pp. 161–430. [CrossRef]
23. Uson, R.; Laguna, A.; Laguna, M.; Briggs, D.A.; Murray, H.H.; Fackler, J.P. (Tetrahydrothiophene)Gold(I) or Gold(III) Complexes. In *Inorganic Syntheses*; Kaesz, H.D., Ed.; John Wiley & Sons, Inc: Hoboken, NJ, USA, 1989; Volume 103, pp. 85–91. [CrossRef]
24. STOE. *X-Area: Single Crystal Diffraction Software*; STOE & Cie GmbH: Darmstadt, Germany, 2019.
25. Koziskova, J.; Hahn, F.; Richter, J.; Kožíšek, J. Comparison of different absorption corrections on the model structure of tetrakis(μ_2-acetato)-diaqua-di-copper(II). *Acta Chim. Slov.* **2016**, *9*, 136–140. [CrossRef]
26. Bruker. *SMART: Program for Bruker CCD X-ray Diffractometer Control*; Bruker: Madison, WI, USA, 2001.
27. Bruker. *SAINT+: Program for Reduction of Data Collected on Bruker CCD Area Detector Diffractometer*; Bruker: Madison, WI, USA, 2009.
28. Bruker. *SADABS: Program for Empirical Absorption Correction of Area Detector Data*; Bruker: Madison, WI, USA, 2008.

29. Sheldrick, G.M. SHELXT—integrated space-group and crystal-structure determination. *Acta Crystallogr.* **2015**, *A71*, 3–8. [CrossRef] [PubMed]
30. Sheldrick, G.M. Crystal structure refinement with SHELXL. *Acta Crystallogr.* **2015**, *C71*, 3–8. [CrossRef]
31. Toby, B.H.; von Dreele, R.B. GSAS-II : The genesis of a modern open-source all purpose crystallography software package. *J. Appl. Crystallogr.* **2013**, *46*, 544–549. [CrossRef]
32. Chen, X.D.; Mak, T.C.W. Order of the coordinating ability of polyatomic monoanions established from their interaction with a disilver(I) metallacyclophane skeleton. *Chem. Commun.* **2005**, *28*, 3529–3531. [CrossRef]
33. Spek, A.L. Structure validation in chemical crystallography. *Acta Crystallogr.* **2009**, *D65*, 148–155. [CrossRef] [PubMed]
34. Kessler, F.; Szesni, N.; Maaß, C.; Hohberger, C.; Weibert, B.; Fischer, H. Transfer of heterocyclic carbene ligands from chromium to gold, palladium and platinum. *J. Organomet. Chem.* **2007**, *692*, 3005–3018. [CrossRef]
35. Williams, D.B.G.; Traut, T.; Kriel, F.H.; van Zyl, W.E. Bidentate amino- and iminophosphine ligands in mono- and dinuclear gold(I) complexes: Synthesis, structures and AuCl displacement by AuC_6F_5. *Inorg. Chem. Commun.* **2007**, *10*, 538–542. [CrossRef]
36. Wimberg, J.; Meyer, S.; Dechert, S.; Meyer, F. Gold(I), Gold(III), and Heterometallic Gold(I)–Silver(I) and Gold(I)–Copper(I) Complexes of a Pyridazine-Bridged NHC/Pyrazole Hybrid Ligand and Their Initial Application in Catalysis. *Organometallics* **2012**, *31*, 5025–5033. [CrossRef]
37. Riedel, D.; Wurm, T.; Graf, K.; Rudolph, M.; Rominger, F.; Hashmi, A.S.K. From Isonitriles to Unsaturated NHC Complexes of Gold, Palladium and Platinum. *Adv. Synth. Catal.* **2015**, *357*, 1515–1523. [CrossRef]
38. Sun, R.W.Y.; Xu, R.F.; Song, H.Q.; Saint-Germain, C.; Zhang, M.; Ni, W.X.; Chen, C.X.; Hemmert, C.; Gornitzka, H.; Li, D. A gold(I)–pyrazolato complex as a switch-on luminescent probe for cysteine: In situ formation of fluorescent nanoparticles and rose-like microspheres. *Inorg. Chem. Front.* **2016**, *3*, 1406–1410. [CrossRef]
39. Authier, A.; Chapuis, G. *A Little Dictionary of Crystallography*; IUCr: Chester, UK, 2014.
40. Chapuis, G.; Authier, A.; Brock, C.P. *Online Dictionary of Crystallography*; IUCr: Chester, UK, 2022.
41. Groom, C.R.; Bruno, I.J.; Lightfoot, M.P.; Ward, S.C. The Cambridge Structural Database. *Acta Crystallogr.* **2016**, *B72*, 171–179. [CrossRef] [PubMed]
42. Sarto, L.E.; Badaró, W.P.D.; de Gois, E.P.; Barbosa, M.I.F.; Torres, C.; Viana, R.B.; Honorato, J.; Castellano, E.E.; de Almeida, E.T. Crystal structures and DFT analysis of Palladium(II) complexes with Schiff bases derived from N,N-dialkyl-*p*-phenylenediamines. *J. Mol. Struct.* **2020**, *1204*, 127549. [CrossRef]
43. Chou, C.C.; Yang, C.C.; Chang, H.C.; Lee, W.Z.; Kuo, T.S. Weaving an infinite 3-D supramolecular network via Au(I)···Au(III) aurophilicity and C–H···Cl hydrogen bonding. *New J. Chem.* **2016**, *40*, 1944–1947. [CrossRef]
44. van Terwingen, S.; Nachtigall, N.; Englert, U. Synthesis and coordination to the coinage metals of a trimethylpyrazolyl substituted 3-arylacetylacetone. *Z. Kristallogr. Cryst. Mater.* **2021**, *237*, 93–99. [CrossRef]